Cranswickite MgSO$_4$·4H$_2$O, a new mineral from Calingasta, Argentina

RONALD C. PETERSON*

Department of Geological Sciences and Geological Engineering, Queen's University, Kingston, Ontario K7L 3N6, Canada

ABSTRACT

Cranswickite is a newly recognized mineral of composition MgSO$_4$·4H$_2$O from Calingasta, San Juan Province, Argentina (IMA2010-016). Cranswickite is monoclinic, space group $C2/c$, a = 11.9236(3), b = 5.1736(1), c = 12.1958(3) Å, β = 117.548(2)°, V = 667.0(1) Å^3, Z = 4, d_{obs} = 1.917 g/cm^3, and d_{calc} = 1.918 g/cm^3. The mineral occurs0 as a soft white vein filling in a metasedimentary rock. The atomic structure has been determined by direct methods and refined by Rietveld analysis of powder diffraction data. The atomic structure consists of chains of corner-sharing magnesium-containing octahedra and sulfate tetrahedra similar to the structure of pentahydrite. All the water molecules directly coordinate magnesium in the structure. The five strongest lines in the powder X-ray diffraction data are [d_{obs} in angstroms (I) (hkl)]: 5.259 (100) (200), 3.927 (46) (11$\bar{2}$), 3.168 (45) (11$\bar{3}$), 4.603 (29) (11$\bar{1}$), 2.570 (23) (311). Infrared and Raman spectra are very similar to the spectra measured from starkeyite. The chemical composition of cranswickite is the same as starkeyite MgSO$_4$·4H$_2$O, but starkeyite has an atomic structure where two sulfate tetrahedra and two Mg(H$_2$O)$_6$ octahedra share corners to form a four-membered ring and not a chain as in cranswickite. The new mineral is named in honor of Lachlan M.D. Cranswick (1968–2010), an Australian crystallographer who helped to developed and maintain the Collaborative Computational Project No. 14 in Powder and Small Molecule Single Crystal Diffraction (CCP14).

Keywords: Cranswickite, starkeyite, pentahydrite, epsomite, meridianiite, chalcanthite, powder diffraction, atomic structure, magnesium sulfate, Argentina

INTRODUCTION

Hydrous magnesium sulfates are commonly found on the surface of the Earth in various settings. The wide variation in the water content from 1 H$_2$O per formula unit in kieserite MgSO$_4$·H$_2$O (Hawthorne et al. 1987) up to 11 H$_2$O per formula unit in meridianiite MgSO$_4$·11H$_2$O (Peterson et al. 2007) allows the stable existence of different hydrous magnesium sulfate minerals over a wide range of temperature, fluid composition, and relative humidity. The phases that are known to exist either in nature or that may be grown in the laboratory are listed in Table 1.

The H$_2$O-MgSO$_4$ phase diagram has been studied extensively (Hogenboom et al. 1995, updated by Chou and Seal 2007; Wang et al. 2006, 2009; Peterson et al. 2007). Cranswickite MgSO$_4$·4H$_2$O, has the same chemical composition as starkeyite MgSO$_4$·4H$_2$O and has an atomic structure similar to pentahydrite MgSO$_4$·5H$_2$O but has not been observed in any experimental synthesis studies. Thermodynamic calculations based on experimental determination of the enthalpies of solution of epsomite, hexahydrite, starkeyite, and kieserite have concluded that starkeyite is metastable in T-%RH space (Grevel and Majzlan 2009). Starkeyite may be metastable, but it is quite commonly found in deposits high in magnesium sulfate on Earth and may exist on the martian surface as a result of dehydration of epsomite at low temperature (Chou and Seal 2007). Chou and Seal (2003) review the literature concerning the epsomite-hexahydrite-vapor equilibrium.

The presence of hydrated magnesium sulfates on the martian

surface is proposed based on observations by the highly successful NASA Mars Exploration Rover Program (Clark et al. 2005) and spectra obtained by several spacecraft orbiting the martian surface (Murchie et al. 2009). Recently the presence of soluble sulfate was observed at the Phoenix landing site (Kounaves et al. 2010). The hydration and dehydration of Mg-sulfates may take place on the surface of Mars where the partial pressure of water vapor is sufficiently high, such as areas where ice is stable in the polar regions or at lower latitudes at times of high obliquity (Vaniman and Chipera 2006; Chipera and Vaniman 2007). It has also been proposed that hydrated sulfate minerals may exist on or below the surfaces of the Jovian moons, Ganymede and Europa (Kargel 1991; Fortes 2005). This is based on spacecraft observation of surficial topography and venting events that may be explained by plate tectonics and hyper saline brine volcanism (Prieto-Ballesteros and Kargel 2005).

Magnesium sulfates have been used in human activities throughout history, as a medicine and naturopathic treatment

TABLE 1. Compounds with the formula MgSO$_4$·nH$_2$O for which the structure is known

Mineral name	Formula	Volume (Å^3)	Z	Reference
Meridianiite	MgSO$_4$·11H$_2$O	702.02	2	Peterson et al. (2007)
Epsomite	MgSO$_4$·7H$_2$O	976.22	4	Baur (1964a)
Hexahydrite	MgSO$_4$·6H$_2$O	1761.17	8	Zalkin et al. (1964)
Pentahydrite	MgSO$_4$·5H$_2$O	364.42	2	Peterson et al. (2006)
Starkeyite	MgSO$_4$·4H$_2$O	636.78	4	Baur (1964b)
Cranswickite	MgSO$_4$·4H$_2$O	667.04	4	This work
2.5 hydrate	MgSO$_4$·2.5H$_2$O	2087.1	16	Ma et al. (2009b)
Sanderite	MgSO$_4$·2H$_2$O	939.16	8	Ma et al. (2009a)
Kieserite	MgSO$_4$·1H$_2$O	355.61	4	Hawthorne et al.(1987)
Anhydrous	MgSO$_4$	266.11	4	Rentzeperis and Soldatos (1958)

* E-mail: peterson@geol.queensu.ca

as well as an industrial chemical. The fact that a new mineral has been found in the $MgSO_4 \cdot nH_2O$ system is indicative of how deceptively complex this binary system is. Metastable existence is possible, and what phases are observed depends on temperature, relative humidity, growth, or dehydration rate, nature of the precursor phase, nucleation limitations, chemical purity, and many other possible factors. Jambor et al. (2000) contains Zayakina and Lazebnik's description of a magnesium sulfate phase that was provisionally called β-starkeyite (UM1999-28-SO:HMg;unnamed 0841, Smith and Nickel 2007). The measured chemical composition is close to $MgSO_4 \cdot 4H_2O$ and the powder diffraction pattern is very similar to that determined for cranswickite (Table 2). Zayakina and Lazebnik (1999) (see Jambor et al. 2000) proposed a triclinic unit cell $a = 7.858(8)$, $b = 13.80(2)$, $c = 5.859(6)$ Å, $\alpha = 90.5°$, $\beta = 92.9°$, $\gamma = 93.0°$, and $V = 634$ Å^3 but the original study material no longer exists and no locality was specified.

The new mineral is named in honor of Lachlan M.D. Cranswick (1968–2010) who, as a crystallographer at the National Research Council of Canada, Canadian Neutron Beam Centre located at Chalk River Laboratories, specialized in applying neutron beams to the study of materials. He assisted many scientists and students from universities across Canada to apply these scientific tools to advance their research programs in materials science, structural chemistry, magnetism, and mineralogy. Lachlan Cranswick was passionate about ensuring the highest quality facilities for those scientists.

Lachlan also made a significant contribution to the application of powder diffraction techniques by helping to develop and maintain the Collaborative Computational Project No. 14 in Powder and Small Molecule Single Crystal Diffraction (CCP14) (Cranswick 2008). The software used to solve the crystal structure of this new mineral was obtained from the CCP14 web site.

The mineral and the name cranswickite have been approved by the International Mineralogical Association, Commission on New Minerals, Nomenclature and Classification (IMA2010-016). Type material has been deposited at the Canadian Museum of Nature (CMNMC 86134).

OCCURRENCE

Cranswickite is found in veins of up to 3 cm in thickness in a fine-grained metasedimetary rock. The rock consists predominately of illite, quartz, and gypsum. The crystal size of the gypsum in the host rock increases to greater than 2 mm close to the veins containing the magnesium sulfate minerals. No magnesium sulfate minerals were detected in the powder diffraction scans of the host rock. The cranswickite occurrence is an outcrop 1 km east-southeast of Calingasta, Argentina (S 31° 20.351′ W 69° 23.546′ elevation 1540 m). There are several small workings where miners have extracted magnesium sulfate, which is purified by dissolution of the ore in water and evaporation of the resulting solution in the dry climate of northern Argentina. Figure 1a shows the nature of the veins within the rock. Some vein material shows coarse interlocking material with a curving morphology, which suggests that the minerals formed in open cavities as the veins extended in width. Figure 1b shows the material on a fractured vein surface. This material consists of a polycrystalline aggregate of very fine crystals of the new mineral cranswickite. The morphology of these curved pseudomorphs suggests that the material grew as another phase and subsequently changed to a polycrystalline aggregate of cranswickite. This morphology is reminiscent of the "rams's horn" morphology sometimes exhibited by gypsum. The identity of this precursor phase is unknown other than it is most likely a higher hydrate of $MgSO_4 \cdot nH_2O$ with n > 4. Elsewhere at the occurrence hexahydrite $MgSO_4 \cdot 6H_2O$ also forms solid veins in the rock. The hexahydrite veins often have a soft surficial dusting of starkeyite that has formed through the dehydration of hexahydrite after the vein has been exposed to the dry, warm atmosphere. At the time of sample collection in December 2009, the air temperature was as high as 38 °C in the late afternoon with a relative humidity of 4%. Sanderite $MgSO_4 \cdot 2H_2O$ and kieserite $MgSO_4 \cdot H_2O$ are also found in the rock debris below the cranswickite occurrence but no information was obtained regarding the spatial associations of these minerals. Cranswickite powder left exposed to a relative humidity of approximately 35% at 298 K in the laboratory hydrated to hexahydrite within two days.

The identification of the new mineral cranswickite and the identification of the associated minerals were made possible by using the "TERRA" portable X-ray diffraction instrument

TABLE 2. Comparison of the powder diffraction data of cranswickite and β-starkeyite (Cu$K\alpha_1$)

h k l	d_{obs}(Å)	I_{obs}(%)	d_{calc} (Å)	I_{calc}(%)	d_{obs}(Å)*	h k l*	I_{obs}(%)*
					6.85	0 2 0	3
					5.85	0 0 1	3
0 0 2	5.387	3	5.395	4	5.41	0 1 $\bar{1}$	10
2 0 0	5.259	100	5.276	100	5.300	$\bar{1}$ 2 0	100
1 1 0	4.603	29	4.639	10	4.622	0 3 0	69
1 1 $\bar{1}$			4.616	30	4.458	0 2 $\bar{1}$	9
1 1 1	3.970	22	3.980	22	3.981	$\bar{1}$ 2 1	60
1 1 $\bar{2}$	3.927	46	3.937	41	3.930	2 0 0	88
1 1 2	3.206	8	3.212	10	3.214	2 1 $\bar{1}$	23
1 1 $\bar{3}$	3.168	45	3.175	35	3.178	2 0 1	93
3 1 $\bar{1}$	3.118	22	3.125	20	3.126	$\bar{2}$ 1 1	62
2 0 2			3.122	19			
3 1 $\bar{2}$			3.104	7			
2 0 $\bar{4}$	3.035	17	3.041	14	3.046	$\bar{2}$ 2 1	50
4 0 $\bar{2}$	2.971	10	2.976	8	2.982	0 4 $\bar{1}$	29
3 1 0	2.904	12	2.910	12	2.916	2 3 0	39
3 1 $\bar{3}$	2.855	5	2.860	5	2.866	0 1 $\bar{2}$	15
0 0 4	2.696	3	2.701	3	2.706	1 4 1	8
4 0 $\bar{4}$	2.570	23	2.575	21	2.576	1 2 $\bar{2}$	62
3 1 1			2.574	21			
1 1 $\bar{4}$			2.573	21			
2 2 1	2.177	3	2.181	3	2.182	3 2 1	11
3 1 $\bar{5}$			2.179	3			
2 2 $\bar{3}$	2.160	3	2.162	3	2.166	$\bar{2}$ 5 1	9
5 1 $\bar{1}$	2.086	2	2.088	2	2.091	$\bar{1}$ 6 1	7
5 1 $\bar{4}$	2.055	1	2.057	1	2.060	1 6 $\bar{1}$	2
2 2 2	1.990	7	1.991	7	1.995	$\bar{2}$ 4 2	18
5 1 0	1.952	14	1.956	10	1.956	$\bar{1}$ 5 2	37
4 2 $\bar{2}$			1.952	13			
5 1 $\bar{5}$	1.912	2	1.914	2	1.918	1 0 $\bar{3}$	6
3 1 6	1.887	4	1.888	4	1.892	3 4 1	14
1 1 5	1.820	2	1.823	2			
1 1 $\bar{6}$	1.804	2	1.808	2			
2 2 $\bar{5}$	1.771	1	1.772	1			
6 0 0			1.761	2			
5 1 $\bar{6}$	1.760	2	1.750	1			
3 1 $\bar{7}$	1.649	2	1.660	1			
4 2 2	1.597	2	1.597	2			
6 2 $\bar{2}$	1.564	2	1.564	3			

Note: We estimate the compound uncertainty of the measured d-values (d_{obs}) to be proportional to the analytically fitted peakwidths as given by its pseudo-Voigt parameters given in Table 5.
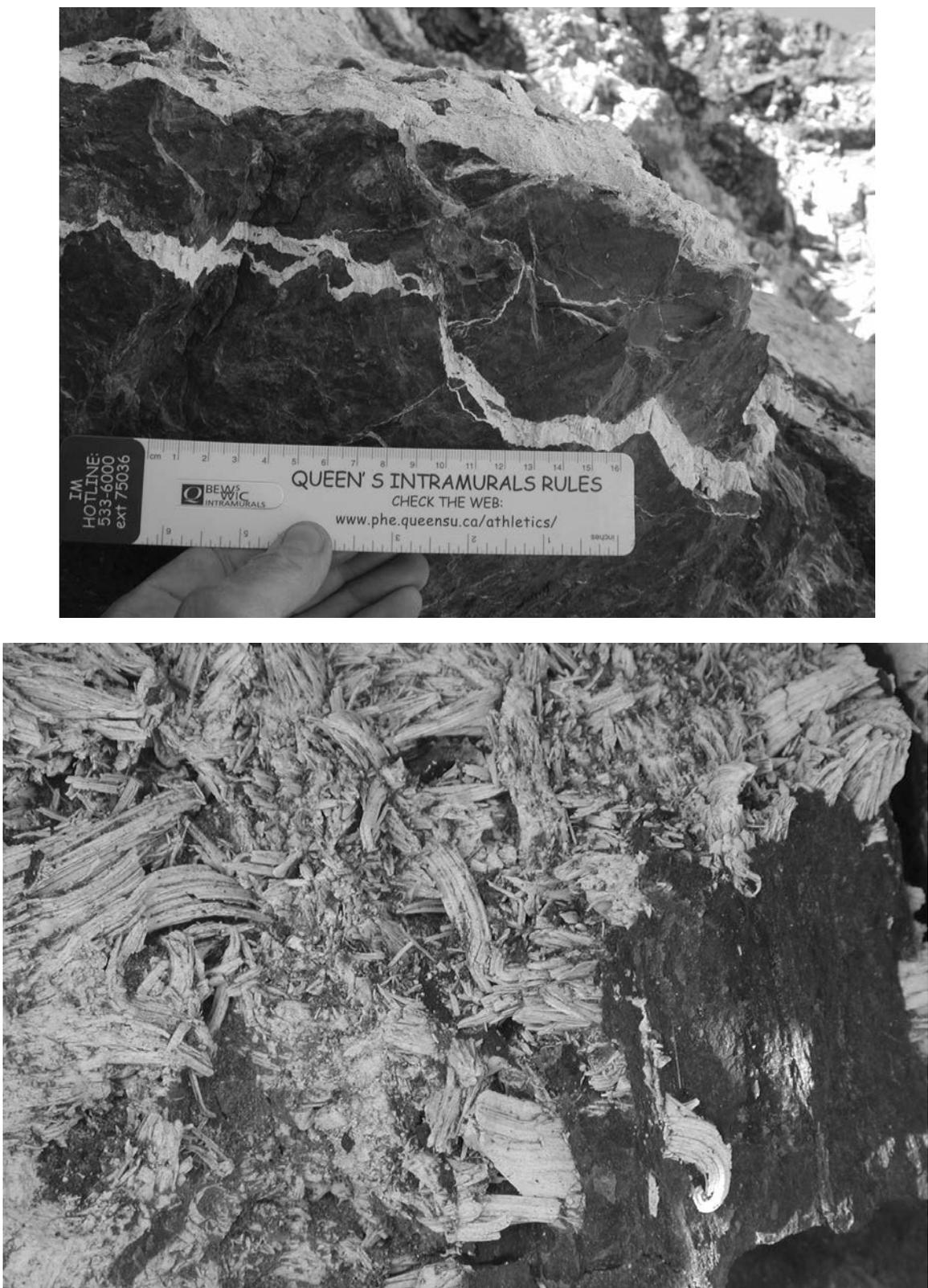* Zayakina and Lazebnik, in Jambor et al. (2000).

Figure 1. (**a**) Veins in rock containing cranswickite. Some veins consist solely of hexahydrite. (**b**) A broken vein surface showing curved fibers. The fibers are a polycrystalline aggregate of very finely crystalline cranswickite. Minor starkeyite also occurs with this material. (Field of view 5 cm.)

(Sarrazin et al. 2008). All of these hydrated magnesium sulfate minerals are soft white powders and are often mixtures. The ability to distinguish these minerals while conducting fieldwork in the remote mountains of Argentina would not have been possible without a portable X-ray diffractometer. The use of a portable diffractometer on location in the field provided immediate information concerning a mineral assemblage and created the opportunity to concentrate on sampling and study without returning to use a laboratory X-ray diffractometer.

PHYSICAL PROPERTIES

Cranswickite occurs as a fine-grained white powder. Very small crystals are visible using a high magnification petrographic microscope and have a maximum dimension of 0.005 mm. The mean refractive index determined using immersion oils of known refractive indices is 1.465 and the Gladstone-Dale compatibility index (Mandarino 2007) is 0.022 (excellent). The density determined using a Berman balance with toluene as the immersion liquid at 20 °C was determined to be 1.917 g/cm^3 (calculated = 1.918 g/cm^3). Starkeyite has a calculated density of 2.01 g/cm^3 due to the slightly smaller unit-cell volume with $Z = 4$ for both minerals. The cranswickite is readily soluble in water. The mineral does not exhibit fluorescence under either the short- or long-wave ultraviolet light.

CHEMICAL COMPOSITION

The water content was determined by heating 0.219 g of sample on a platinum tray to 450 °C for 2 h in air. The weight loss was 0.083 g or 37.9% and corresponds to $MgSO_4 \cdot 4.07H_2O$. A search of the X-ray fluorescence spectrum measured with an Oxford EDS detector and an AMRAY 1830 scanning electron microscope operating at 20 kV, yielded no other X-ray peaks beside those of O, S, and Mg using a 200 s counting time. Chemical analysis by ICP-MS was performed. 0.1 g of sample was weighed into a disposable SCP science digitube and dissolved into 50 mL of distilled water. Magnesium sulfate (certified ACS grade, $MgSO_4 \cdot 7H_2O$) was analyzed in duplicate as a control. The results are presented in Table 3.

INFRARED SPECTROSCOPY

The infrared spectrum of cranswickite was measured using a Nicolet Avatar 320 FTIR spectrometer. We performed 32 scans over the range of 4 to 4000 cm^{-1} with 4 cm^{-1} resolution. The spectrum is presented in Figure 2. The spectra of starkeyite and cranswickite are quite similar. There is a difference in the 700 cm^{-1} wavenumber region of the spectra, which may be attributed to differences in the asymmetric bending frequencies of the SO_4

tetrahedra due to the ring structure of starkeyite vs. the chain structure of cranswickite.

Raman spectroscopy was performed with a HORIBA/Jobin Yvon (Edison, New Jersey) micro-Raman spectrometer (Model: LabRAM), equipped with a 632 nm He/Ne laser source, 1800 g/mm grating, and an Olympus BX41 microscope system. Collection of spectra was performed in the backscattered mode at 25 °C using the following settings: ×100 microscope objective, 500 µm pinhole size, and 5 µm slit width. The software LabSpec 4.1 was used for data processing. Data acquisition times in the range 10–30 s were used depending on the sample examined and corresponding resolution of the collected spectrum. Cranswickite and starkeyite samples were measured twice under the same conditions and each reported spectrum represents the average of two measurements. The samples were transferred from their sealed containers and placed in the spectrometer and the spectra measured within two minutes. The spectra are presented in Figure 3. The main peaks of the Raman shift for cranswickite and starkeyite are very similar in shape and position, and the observed maximum of 1001.6 cm^{-1} is very close to that observed for starkeyite by Wang et al. (2006) of 1000.3 cm^{-1}. Table 4 lists the suggested assignments for the infrared and Raman spectra.

X-RAY DIFFRACTION

Cranswickite is often intimately mixed with hexahydrite, starkeyite, and/or kieserite. One sample contained no other phases and was used for further study. The sample was ground with a mortar and pestle, back-packed into a sample holder, and scanned using a Panalytical X'pert Pro diffractometer equipped with a copper-target X-ray tube operating at 40 kV and 45 mA, incident slit of 1/16 degree with a 1/8 degree anti-scatter slit and 0.02 rad. Soller slits. A diffracted-beam graphite monochromator (Johansson type Alpha-1 geometry) was used and the diffracted X-rays were detected with an X'celerator position sensitive

FIGURE 2. Comparison of the FTIR spectra of the cranswickite, starkeyite, and water measured at room temperature in air. In the regions of water absorption, the downward shift of the stretching band (near 3300 cm^{-1}) and the upward shift of the bending band (near 1650 cm^{-1}) are indications of stronger hydrogen bonding in cranswickite than in starkeyite.

TABLE 3. Chemical composition determined by ICP-MS

	Conc. µg/g	Element/per 1 S*	wt%
Co	97.3	0.0003	0.01
Mg	122000	0.9863	20.28
Mn	446	0.0016	0.06
Ni	605	0.0020	0.08
S	165000	1	41.59
Zn	1370	0.0041	0.17
H$_2$O			37.90

* Estimated error for magnesium is 0.98(2). Cobalt, manganese, and zinc are included as their concentrations were significantly above the detection limits of the ICP-MS but present in trace amounts.
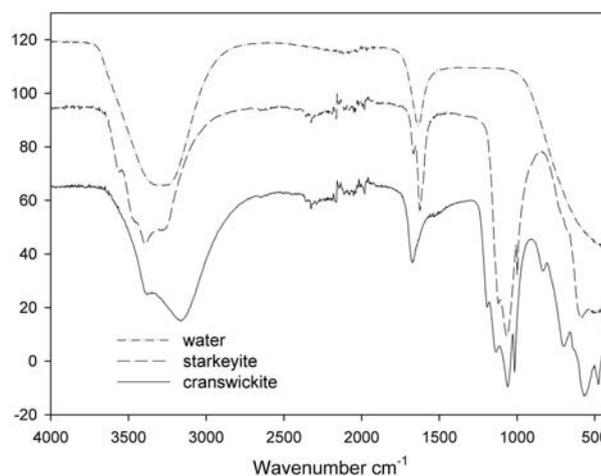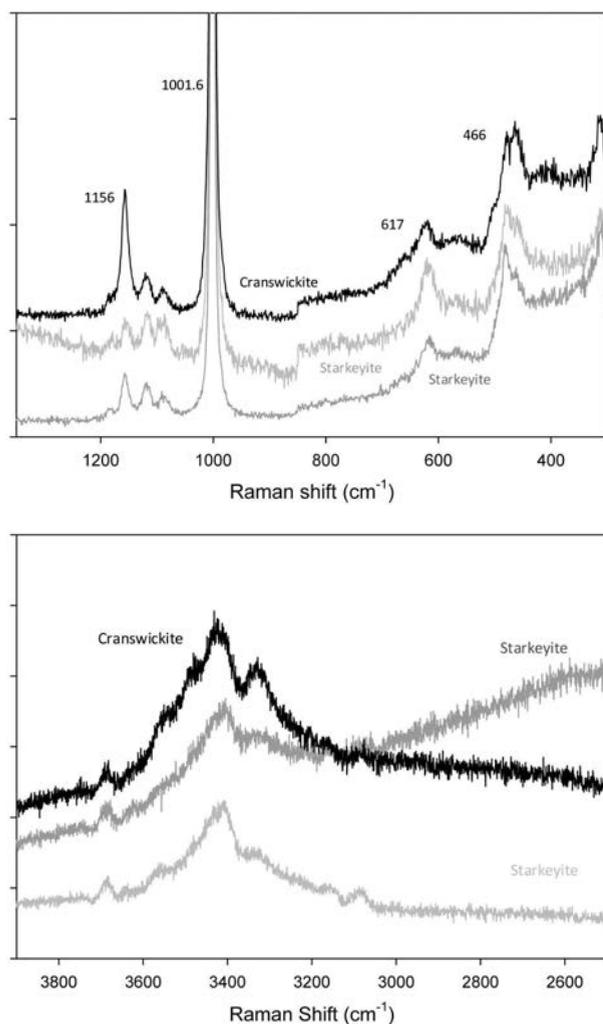
FIGURE 3. The Raman spectra of cranswickite and two specimens of starkeyite from the cranswickite locality. The spectra are very similar but the peak at 1156 cm⁻¹ due to anti-symmetric SO_4 stretchingis more intense in cranswickite. The very strong peak at peak at approximately 1001 cm⁻¹ due to symmetric SO_4 stretching is very similar in these minerals.

TABLE 4. Wavenumbers (cm⁻¹)* observed in the infrared and Raman spectra of cranswickite

IR	Raman	Suggested assignments and comments
~3375 S,sh	~3430 w	Stretching modes of H_2O molecules
~3290 VS,broad	~3300 vw	
1674 m	–	Bending mode of H_2O molecules
~1192 m,sh	1156 m	Degenerate (F_2) SO_4 stretching mode several components due to crystal splitting
1136 S,sh	1120 w	
1060 VS,broad	1090 vw	
1016 S,sharp	–	
Inactive	1002 VS, sharp	Symmetric (A_1) SO_4 stretching mode
833 w	–	Lattice vibrations involving water molecules
700 m	–	
–	617 w	Degenerate (F_2) SO_4 bending mode
563 VS	–	Mg-O stretching modes of H2O coordinated magnesium ions
477 S	–	
Inactive	466 w	Degenerate (E) SO_4 bending mode

* Relative intensities are denoted by: VS = strong, S = strong, m = medium, w = weak, vw = very weak, sh = shoulder.

detector. Data were collected from 4 to 85 °2θ with an effective step size of 0.017 °2θ and a 400 s counting time. The peaks in the powder diffraction pattern are listed in Table 2. Figure 4 presents the experimentally determined X-ray diffraction spectra of cranswickite and starkeyite.

The diffraction data of cranswickite were analyzed using the program EXPO2009 (Altomare et al. 2009). The peaks were identified and indexed by N-TREOR (Altomare et al. 2000) and the atomic structure was determined by direct methods using EXPO2009. The space group was determined to be $C2/c$ based on the unit-cell dimensions and systematic extinctions that were observed. The resulting model was then refined using the program HIGHSCORE (vers. 2.2, Panalytical 2008). Background was modeled using a fourth-order polynomial and a pseudo-Voigt function was used to model peak shape. Table 5 presents the details of the Rietveld refinement, Table 6 lists the atomic coordinates, and Figure 5 shows the calculated and observed profiles of the Rietveld refinement. The unit-cell volume is 667.0(1) Å³, which is close to the volume of starkeyite as determined by Baur (1964b) (636.8 Å³). Individual isotropic atomic displacement parameters were refined, and the hydrogen positions were not determined. Bond lengths and angles between selected bonds are given in Table 7.

ATOMIC STRUCTURE

The atomic structure of cranswickite consists of chains of alternating sulfate tetrahedra and magnesium-containing octahedra. A CIF is on deposit[1]. Coordination about the magnesium is by four water molecules and two oxygen atoms that are shared with sulfate tetrahedra. Oxygen atoms of the sulfate

---

[1] Deposit item AM-11-026, CIF. Deposit items are available two ways: For a paper copy contact the Business Office of the Mineralogical Society of America (see inside front cover of recent issue) for price information. For an electronic copy visit the MSA web site at http://www.minsocam.org, go to the *American Mineralogist* Contents, find the table of contents for the specific volume/issue wanted, and then click on the deposit link there.

TABLE 5. Rietveld refinement details

a (Å)	11.9236(3)
b (Å)	5.1736(1)
c (Å)	12.1958(3)
β (°)	117.548(2)
V (Å³)	667.0(1)
R_{exp} (%)	6.52
R_p (%)	7.53
R_{wp} (%)	9.94
GOF	2.32
R_{Bragg} (%)	3.39
U	0.47(2)
V	−0.066(8)
W	0.0168(9)

TABLE 6. Fractional atomic coordinates and isotropic displacement parameters

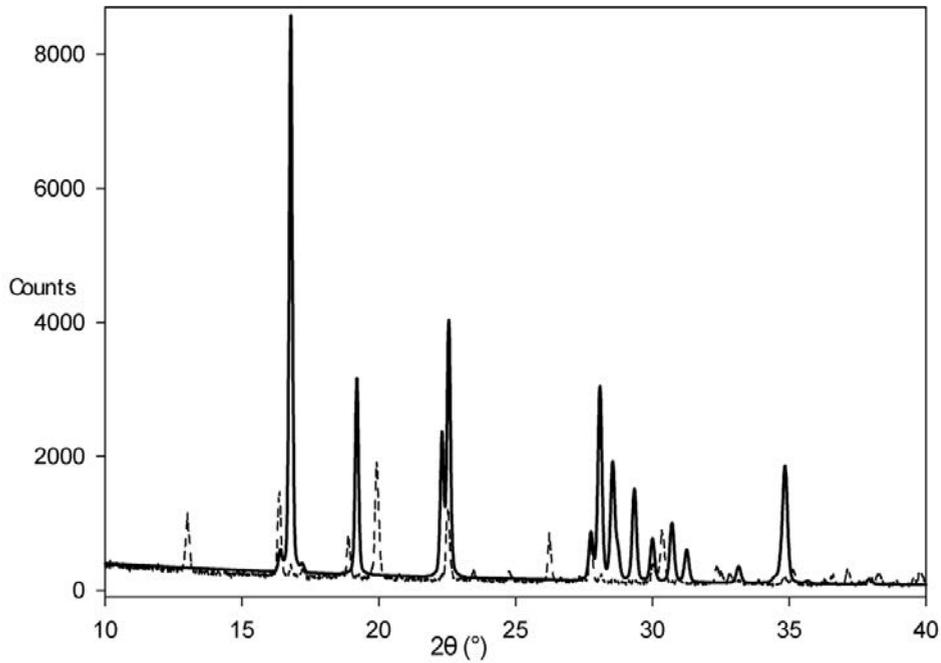| Atom	x	y	z	B_{iso}
S	0	0.3131(4)	3/4	1.57(7)
Mg	0	0	1/2	1.19(8)
O1	0.1165(3)	0.5160(5)	0.2925(3)	2.1(1)
O2	0.9834(3)	0.1424(8)	0.6456(3)	2.3(1)
O3	0.8759(2)	0.7094(6)	0.4976(3)	0.95(9)
O4	0.8543(2)	0.2347(6)	0.3732(3)	0.37(9)

FIGURE 4. Comparison of the powder X-ray diffraction spectra of cranswickite and starkeyite. The dark line is cranswickite data and the dashed line is starkeyite. Both data sets were obtained with monochromatized $CuK\alpha_1$ radiation.
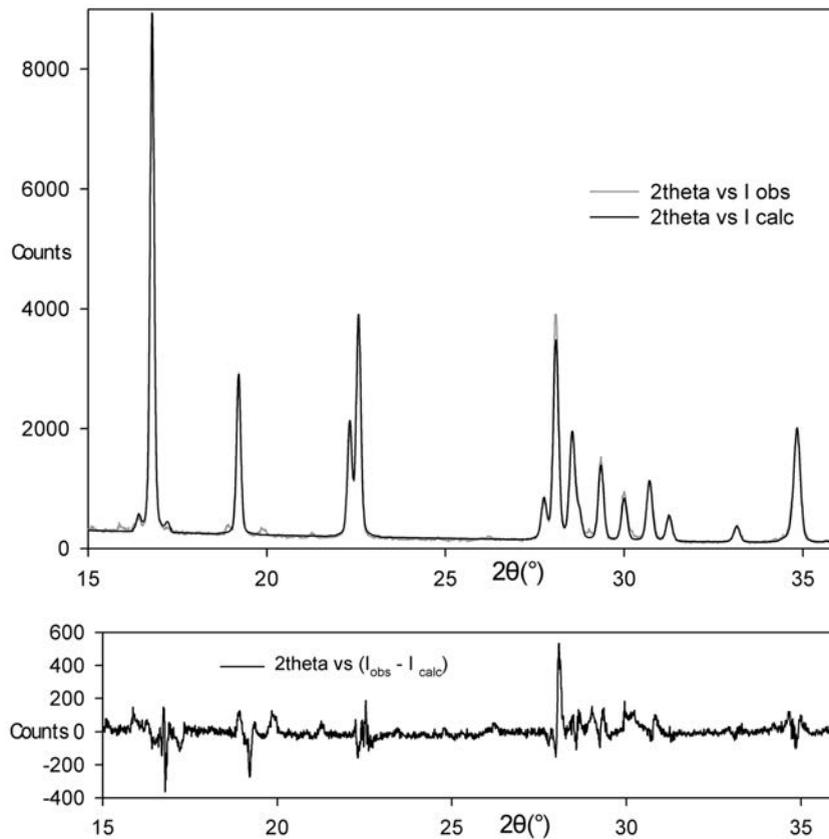

FIGURE 5. Calculated (dark) and observed (light gray) profiles and their difference for the Rietveld refinement.

group act as a hydrogen bond acceptor. This atomic linkage is the same as that observed in pentahydrite $MgSO_4 \cdot 5H_2O$ (Baur and Rolin 1972), chalcanthite $CuSO_4 \cdot 5H_2O$ (Bacon and Titterton 1975), and siderotil $FeSO_4 \cdot 5H_2O$ (Peterson et al. 2003). The additional water molecule in pentahydrite, chalcanthite, and siderotil occurs between the chains and is held in place by hydrogen bonds. All of these minerals have chains that are formed by the alternation of sulfate tetrahedra and magnesium (or iron)-containing octahedra (Figs. 6a and 6b). The $S-M^{+2}-S$ angles in all three structures are 180° (Table 8). The main difference in the three structures is the chain periodicity, which is 12.2 Å in cranswickite and 10.8 Å in pentahydrite and siderotil. This longer chain in the cranswickite atomic structure also results in $M^{2+}-S-M^{2+}$ angles that are larger in cranswickite (124°) and less in siderotil and pentahydrite (103°,105°) as well as larger $M^{2+}-O-S$ angles in cranswickite (Table 8). The structure of cranswickite $MgSO_4 \cdot 4H_2O$ is different than the structures of starkeyite $MgSO_4 \cdot 4H_2O$ and rozenite $FeSO_4 \cdot 4H_2O$ where the sulfate tetrahedra and magnesium-containing octahedra share corners to make a four-membered ring instead of a chain (Fig. 6c). Sulfate tetrahedra are linked to the magnesium-containing octahedra in a *trans* fashion in cranswickite (Fig. 6a) as opposed to a *cis* fashion in starkeyite (Fig. 6c).

Transformation between the 6, 7, and 11 hydrates involves no changes in linkages between sulfate tetrahedra and magnesium octahedra because no direct links exist between the polyhedra in these structures. In pentahydrite and lower hydrates, there are connections between the tetrahedra and octahedra, and transformation from one structure to another requires disruption or formation of these polyhedral linkages on hydration or dehydration. In the case of a possible dehydration from pentahydrite to cranswickite, there would be no disruption or formation of linkages between tetrahedra and octahedra. Only the breaking of hydrogen bonds and the diffusion of water molecules out of the atomic structure is required. Figure 7 shows the similarity between cranswickite and pentahydrite. Both consist of similar chains of magnesium-containing octahedra and sulfate tetrahedra, but pentahydrite has a water molecule that is not bonded directly to a magnesium atom and occurs between the chains.

Figure 8 shows the volume of the unit cell for the various hydration states of $MgSO_4$, normalized to $Z = 1$, vs. the number of water molecules. The linear regression gives a slope of 25.8
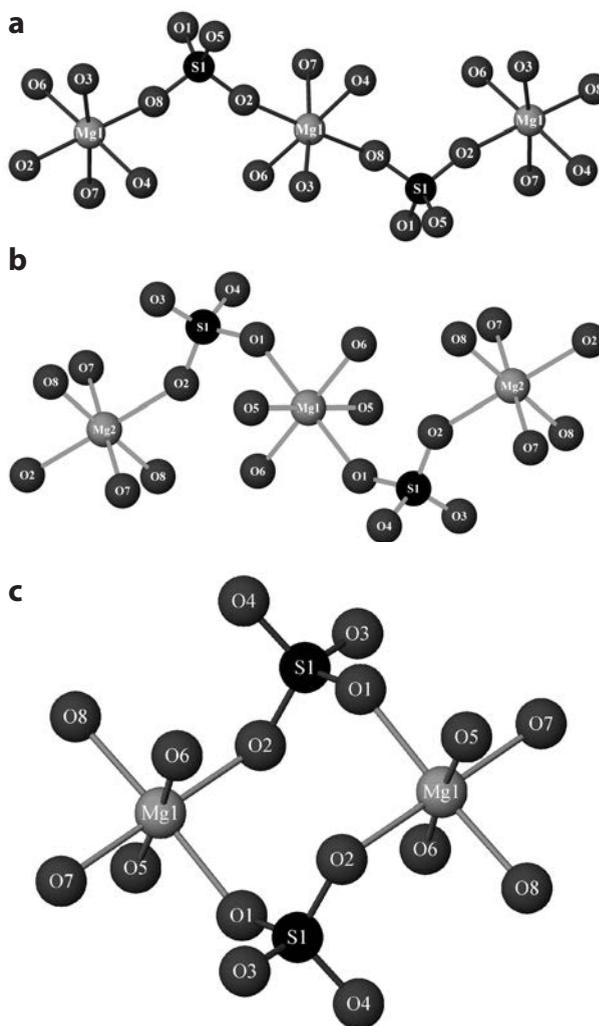

FIGURE 6. Comparison of the chains of alternating $MgO_2(H_2O)_4$ octahedra and SO_4 tetrahedra in (**a**) cranswickite and (**b**) pentahydrite. The chain periodicity is 12.2 Å in the cranswickite and 10.8 Å in pentahydrite even though the polyhedra are of similar size. This is due to the increased kinking of the chain in pentahydrite (Table 8). The starkeyite structure (**c**) consists of four-membered rings instead of chains.

$Å^3$ for the effective volume increase for each water molecule added. It is surprising that the fit to a linear trend is so good considering that for the lower hydrated structures the water molecules are directly involved in the coordination of the magnesium, whereas for the magnesium sulfate minerals with higher degrees of hydration many of the water molecules are not directly bonded to a magnesium atom and are held in place solely by hydrogen bonds.
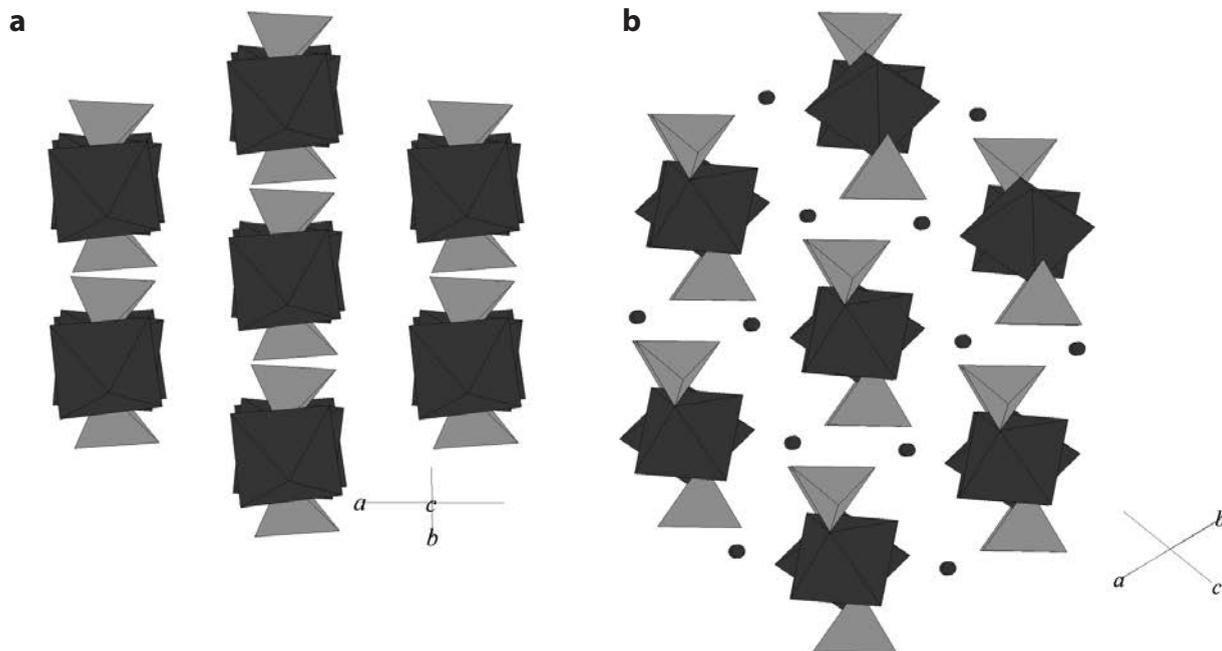
TABLE 7. Bond lengths (Å) and angles (°) in cranswickite

S-O1	1.521(4)	x2	Mg-O2	2.015(4)	x2	O2-Mg-O3	94.7(2) x2
S-O2	1.486(4)	x2	Mg-O3	2.100(3)	x2	O2-Mg-O3	85.3(2) x2
Mean	1.504		Mg-O4	2.097(3)	x2	O2-Mg-O4	91.5(2) x2
			Mean	2.071		O3-Mg-O4	88.3(1) x2
O1-S-O1	108.9(4)					O3-Mg-O4	91.7(2) x2
O1-S-O2	108.3(4)					O4-Mg-O2	88.5(2) x2
O1-S-O2	108.3(4)						
O1-S-O2	112.1(4)						
O1-S-O2	112.1(4)						
O2-S-O2	107.1(4)						

TABLE 8. Comparison of the unit-cell volumes and dimensions of the octahedra-sulfate tetrahedra chains in related structures

	Cranswickite	Pentahydrite	Chalcanthite	Siderotil
Unit cell vol. (Z = 4 equiv.) (Å³)	667.0(1)	728.8	732.8	736.0
Chain periodicity (Å)	12.1958(3)	10.81	11.14	10.84
$M^{2+}-S-M^{2+}$ angle (degrees)	124.0(8)	104.9	100.6	103.2
$M^{2+}-O-S$ angle (degrees)	161(1)	144/143	139/132	139/138
$S-M^{2+}-S$ angle (degrees)	180	180	180	180

FIGURE 7. Comparison of the crystal structures of (**a**) cranswickite and (**b**) pentahydrite. This projection is along the chains of alternating octahedra and tetrahedra. The water molecules not involved in coordinating magnesium atoms in pentahydrite are shown as spheres. The topology of these two structures is very similar and as the water is removed from the pentahydrite structure (**b**) the chains move closer together and become straighter in cranswickite (**a**). In these drawings, tone can see that the chains made up of sulfate tetrahedra with magnesium octahedra are more linear in cranswickite.
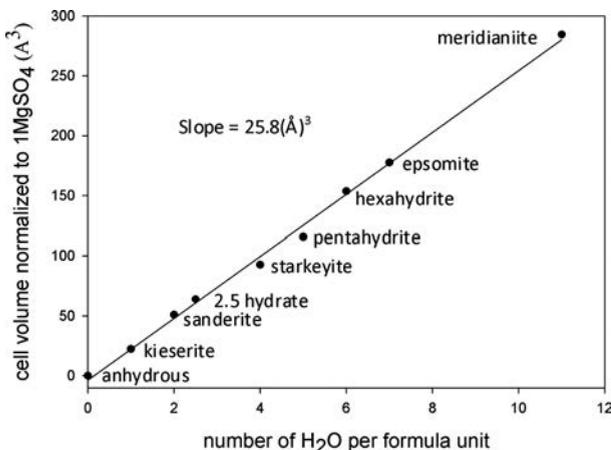
FIGURE 8. The number of water molecules for each $MgSO_4$ vs. the unit-cell volume (normalized to $Z = 1$ $MgSO_4 \cdot nH_2O$). This linear trend has a slope of 25.3 $Å^3$ and corresponds to an effective sphere for the water molecule with a radius of 1.82 Å.

REFERENCES CITED

Altomare, A., Giacovazzo, C., Guagliardi, A., Moliterni, A.G.G., Rizzi, R. and Werner, P. E. (2000) New techniques for indexing: *N-TREOR* in *EXPO*. Journal of Applied Crystallography, 33, 1180–1186.
Altomare, A., Camalli, M., Cuocci, C., Giacovazzo, C., Moliternia, A., and Rizzia, R. (2009) EXPO2009: structure solution by powder data in direct and reciprocal space. Journal Applied Crystallography, 42, 1197–1202.
Bacon, G.E. and Titterton, D.H. (1975) Neutron diffraction studies of $CuSO_4 \cdot 5(H_2O$ and $CuSO_4 \cdot 5(D_2O)$. Zeitschrift für Kristallographie, 141, 330–341.
Baur, W.H. (1964a) On the crystal chemistry of salt hydrates; Part 4, The refinement of the crystal structure of $MgSO_4 \cdot 7H_2O$ (epsomite). Acta Crystallographica, 17, 1361–1369.
——— (1964b) On the crystal chemistry of salt hydrates; Part 2, A neutron diffraction study of $MgSO_4 \cdot 4H_2O$. Acta Crystallographica, 17, 863–869.
Baur, W.H. and Rolin, J.L. (1972) Salt hydrates. IX. The comparison of the crystal structure of magnesium sulfate pentahydrate with copper sulfate pentahydrate and magnesium chromate pentahydrate. Acta Crystallographica, B28, 1448–1455.
Clark, B., Morris, R., McLennan, S., Gellert, R., Jolliff, B., Knoll, A., Squyres, S., Lowenstein, T., Ming, D., Tosca, N., and others. (2005) Chemistry and mineralogy of outcrops at Meridiani Planum. Earth and Planetary Science Letters, 240, 73–94.
Cranswick, L.M.D. (2008) Computer software for powder diffraction. In R.E. Dinnebier and S.J.L. Billinge, Eds., Powder Diffraction Theory and Practice, p. 494–570. RCS Publishing, Cambridge.
Chipera, S.J. and Vaniman, D.T. (2007) Experimental stability of magnesium sulfate hydrates that may be present on Mars. Geochimica et Cosmochimica Acta, 71, 241–250.
Chou, I. and Seal, R. (2003) Determination of epsomite-hexahydrite equilibria by the humidity-buffer technique at 0.1 MPa with implications for phase equilibria in the system $MgSO_4 \cdot H_2O$. Astrobiology, 3, 619–630.
——— (2007) Magnesium and calcium sulfate stabilities and the water budget of Mars. Journal of Geophysical Research, 112, e11004.
Fortes, A.D. (2005) From Surrey to the moons of Jupiter (via Mars): the story of Epsomite. Axis, 1, 1–28.
Grevel, K. and Majzlan, J. (2009) Internally consistent thermodynamic data

for magnesium sulfate hydrates. Geochimica et Cosmochimica Acta, 73, 6805–6815.

Hawthorne, F.C., Groat, L.A., Raudsepp, M., and Ercit, T.S. (1987) Kieserite, $Mg(SO_4)\cdot H_2O$, a titanite-group mineral. Neues Jahrbuch für Mineralogie, Abhandlungen, 157, 121–132.

Hogenboom, D.L., Kargel, J.S., Ganasan, J.P., and Lee, L. (1995) Magnesium sulfate-water to 400 MPa using a novel piezometer: Densities, phase equilibria, and planetological implications. Icarus, 115, 258–277.

Jambor, J.L., Grew, E.S. and Roberts, A.C. (2000) New mineral names. American Mineralogist, 85, 1561–1565.

Kargel, J.S. (1991) Brine volcanism and the interior structures of icy satellites. Icarus, 94, 368–390.

Kounaves, S., Hecht, M., Kapit, J., Quinn, R., Catling, D., Clark, B., Ming, D., Gospodinova, K., Hredzak, P. McElhoney, K., and Shusterman, J. (2010) Confirmation of soluble sulfate at the Phoenix landing site: Implications for Martian geochemistry and habitability. 41st Lunar and Planetary Science Conference, Abstract 2199.

Ma, H., Bish, D.L., Wang, H., and Chipera, S. (2009a) Determination of the crystal structure of sanderite, $MgSO_4\cdot2H_2O$, by X-ray powder diffraction and the charge flipping method. American Mineralogist, 94, 622–625.

——— (2009b) Structure determination of the 2.5 hydrate $MgSO_4$ phase by simulated annealing. American Mineralogist, 94, 1071–1074.

Mandarino, J.A. (2007) The Gladstone-Dale compatibility of minerals and its use in selecting mineral for further study. Canadian Mineralogist, 45, 1307–1324.

Murchie, S., Arvidson, R., Bedini, P., Beisser, K., Bibring, J.-P., Bishop, J., Boldt, J., Cavender, P., Choo, T., Clancy, R.T. and others. (2009) Compact Reconnaissance Imaging Spectrometer for Mars investigation and data set from the Mars Reconnaissance Orbiter's primary science phase. Journal of Geophysical Research, 114, E00D07.

Peterson, R.C., Roeder, P.L., and Yousheng, Z. (2003) The atomic structure of siderotil, $(Fe, Cu)SO_4\cdot5H_2O$. Canadian Mineralogist, 41, 671–676.

Peterson, R.C., Hammarstrom, J.M., and Seal, R. (2006) Alpersite (Mg,Cu) $SO_4\cdot7H_2O$, a new mineral of the melanterite group, and cuprian pentahydrite: Their occurrence within mine waste. American Mineralogist, 91, 261–269.

Peterson, R.C., Nelson, W., Madu, B. and Shurvell, H.F. (2007) Meridianiite: a new mineral species observed on Earth and predicted to exist on Mars. American Mineralogist, 92, 1756–1759.

Prieto-Ballesteros, O. and Kargel, J. (2005) Thermal state and complex geology of a heterogeneous salty crust of Jupiter's satellite, Europa. Icarus, 173, 212–221.

Rentzeperis, P.J. and Soldatos, C.T. (1958) The crystal structure of the anhydrous magnesium sulfate. Acta Crystallographica, 11, 686–688.

Sarrazin, P., Brunner, W., Blake D., Gailhanou, M., Bish, D.L., Vaniman, D., Chipera, S., Ming, D.W., Steele, A., Midtkandal, I., Amundsen, H.E.F. and Peterson, R. (2008) Field studies of Mars analog materials using a portable XRD/XRF instrument, Lunar and Planetary Science Conference XXXX, Lunar and Planetary Institute, Houston, Texas.

Smith, D.G.W. and Nickel, E.H. (2007) A system of codification for unnamed minerals: Report of the Subcommittee for Unnamed Minerals of the IMA Commission on New Minerals, Nomenclature and Classification. Canadian Mineralogist, 45, 983–1055.

Vaniman, D. and Chipera, S. (2006) Transformations of Mg- and Ca-sulfate hydrates in Mars regolith. American Mineralogist, 91, 1628–1642.

Wang, A., Freeman, J., Jolliff, B., and Chou, I. (2006) Sulfates on Mars: A systematic Raman spectroscopic study of hydration states of magnesium sulfates. Geochimica et Cosmochimica Acta, 70, 6118–6135.

Wang, A., Freeman, J., and Jolliff, B. (2009) Phase transition pathways of hydrates of magnesium sulfate in the temperature range 50 to 5 °C: implication for sulfates on Mars. Journal of Geophysical Research, 114, E04010, DOI: 10.1029/2008JE003266.

Zalkin, A., Ruben, H., and Templeton, D.H. (1964) The crystal structure and hydrogen bonding of magnesium sulfate hexahydrate. Acta Crystallographica, 17, 235–240.

Zayakina, N.V. and Lazebnik, K.A. (1999) Tetrahydrate magnesium sulfate from western Yakutiya. Zapiski. Vseross. Mineral. Obshch, 128(4), 99–101.